

# Structure and viscoelastic properties of amorphous ethylene/1-hexene copolymers obtained with metallocene catalyst

H. Miyata<sup>a,b</sup>, M. Yamaguchi<sup>a</sup>, M. Akashi<sup>b,\*</sup>

<sup>a</sup>Yokkaichi Research Laboratory, TOSOH Corporation, 1-8 Kasumi, Yokkaichi, Mie 510-8540, Japan

<sup>b</sup>Department of Applied Chemistry and Chemical Engineering, Faculty of Engineering, Kagoshima University, 1-21-40 Korimoto, Kagoshima 890-0065, Japan

Received 7 August 2000; received in revised form 24 November 2000; accepted 11 December 2000

## Abstract

Copolymerization of ethylene and 1-hexene was performed with diphenylmethyldiene (cyclopentadienyl-fluorenyl) zirconium dichloride ( $\text{Ph}_2\text{C}(\text{Cp})(\text{Flu})\text{ZrCl}_2$ ) in combination with dimethylanilinium tetrakis-(pentafluorophenyl)borate ( $(\text{Me}_2\text{PhNH})(\text{B}(\text{C}_6\text{F}_5)_4)$ )/triisobutylaluminum ( $i\text{-Bu}_3\text{Al}$ ) catalyst. This catalyst system produced ethylene/1-hexene random copolymers (EHRs) with high molecular weight and narrow molecular weight distribution. The rheological properties of the rubbery EHRs were compared with those of the rubbery ethylene/propylene copolymer (EPR). It was found that the rubbery plateau modulus  $G_N^0$  of the EHR is much lower than that of the EPR. © 2001 Published by Elsevier Science Ltd.

**Keywords:** Ethylene/propylene rubber; Ethylene/hexene rubber; Metallocene catalyst

## 1. Introduction

After the frontier works by Kaminsky [1], great interest has arisen in the field of metallocene catalyst technology. In particular, there have been many reports on the copolymerization of ethylene and  $\alpha$ -olefins [2–5]. Kaminsky and Miri [2] showed that dicyclopentadienyl zirconium dimethyl ( $\text{Cp}_2\text{ZrMe}_2$ )/methylaluminoxane (MAO) has high activity for the copolymerization of ethylene and propylene and the terpolymerization of ethylene, propylene, and 5-ethylidene-2-norbornene. Moreover, the catalyst system was found to produce the random polymers having narrow molecular weight distribution. Further, Ewen [3] studied the reactivity ratio for several metallocene catalysts. Chien and He [4] investigated the relation between metal centers of the metallocene compounds and the characteristics of the copolymers obtained. Uozumi and Soga [5] discussed the effect of the catalyst stereospecificity on the copolymerization reactivity for the ethylene/propylene and ethylene/1-hexene copolymerization.

Their intensive studies make it possible to produce various kinds of rubbery ethylene/ $\alpha$ -olefin copolymers commercially. Thus, much attention has been focused on the application of the vulcanized rubber. Mäder et al. [6]

studied the thermal properties of the rubbery ethylene/ $\alpha$ -olefin copolymers produced by the metallocene catalyst, in which the copolymers having below 50 mol% of  $\alpha$ -olefin were used. According to them, glass transition temperature  $T_g$  takes the lowest value when the  $\alpha$ -olefin content in the copolymer is about 50–60 wt% for both rubbery ethylene/propylene copolymer (EPR) and ethylene/1-butene copolymer (EBR). The results agree well with those obtained by the model EBR produced by the hydrogenation of polybutadienes with various vinyl contents [7]. Moreover, the rheological properties of the model EBRs were investigated by Carella et al. [7]. According to them, the rubbery plateau modulus  $G_N^0$  decreases with increasing 1-butene content in the EBR, whereas the product of  $J_e^0 G_N^0$  is constant, where  $J_e^0$  represents the steady-state compliance. The rheological properties of rubbery ethylene/1-hexene copolymer (EHR) and ethylene/1-octene copolymer (EOR), however, have not been clarified yet, although both EBR and EOR can be produced by the metallocene catalyst. Furthermore, it is important for the industrial application because the rheological properties greatly affect the processability as well as the mechanical properties of the vulcanized rubbers.

The aim of this study is to clarify the characteristics of the rubbery EHR produced by the metallocene catalyst system composed of diphenylmethyldiene (cyclopentadienyl-fluorenyl) zirconium dichloride ( $\text{Ph}_2\text{C}(\text{Cp})(\text{Flu})\text{ZrCl}_2$ ) in combination with dimethylanilinium tetrakis-(pentafluorophenyl)

\* Corresponding author. Tel.: +81-99-285-8320; fax: +81-99-255-1229.  
E-mail address: akashi@apc.kagoshima-u.ac.jp (M. Akashi).

borate ( $[\text{Me}_2\text{PhNH}][\text{B}(\text{C}_6\text{F}_5)_4]$ )/triisobutylaluminum ( $i\text{-Bu}_3\text{Al}$ ). In this paper, we will discuss the relation between molecular characteristics of the EHR and mechanical properties of the vulcanized EHR.

## 2. Experimental

### 2.1. Materials

$\text{Ph}_2\text{C}(\text{Cp})(\text{Flu})\text{ZrCl}_2$  was synthesized according to the literature [8].  $[\text{Me}_2\text{PhNH}][\text{B}(\text{C}_6\text{F}_5)_4]$  and  $i\text{-Bu}_3\text{Al}$  from Tosoh Akzo Co. were used without purification. Ethylene, 1-hexene, and toluene as a solvent were obtained commercially and purified according to the usual procedures.

### 2.2. Copolymerization procedure

The copolymerization was carried out in a 5-l stainless steel autoclave equipped with a temperature controller and a magnetic stirrer. The autoclave was filled with 2.5 l of toluene containing 1-hexene and heated up to 313 K. Then ethylene was supplied into the autoclave to a total pressure of 0.4 MPa. The polymerization was initiated by adding the catalyst. The polymerization took 10 min. The temperature was kept at 313 K, and ethylene was fed through the autoclave continuously during the polymerization. The highest conversion of 1-hexene was less than 10% in this study. The polymerization was terminated by adding ethanol. After the autoclave was degassed, the polymer solution was precipitated with ethanol. Then the precipitated polymer was washed with ethanol several times and dried in vacuum at 353 K. In the case of the copolymerization with propylene as a comonomer, ethylene and propylene were continuously supplied into the autoclave.

In this study, four kinds of EHRs and one EPR were prepared. The nomenclature of copolymers is as follows; e.g. EHR25 is ethylene/1-hexene copolymer containing 25 mol% 1-hexene.

### 2.3. Characterization of copolymers

The contents of 1-hexene and triad sequence distributions of the copolymers were determined by  $^{13}\text{C}$  NMR. The spectra were recorded with a JEOL GX-400 spectrometer operating at 100 MHz. Measurements were carried out for

5–10 wt/vol% of the copolymer solution in *ortho*-dichlorobenzene/benzene- $\text{d}_6$  (vol. ratio = 9:1) at 403 K. The number of branches was calculated according to the method of Randall [9].

The number-, weight-, and  $z$ -average molecular weights were determined by means of a combination of gel permeation chromatography (GPC) (Waters 150-C ALC/GPC instrument equipped with TOSOH mixed bed columns) and on-line intrinsic viscosity measurements (Viscotek, Differential Viscometer Model 100) in which *ortho*-dichlorobenzene was used as the solvent. Universal calibration procedures were used in order to estimate the molecular weights [10]. Moreover, the monomer composition of the copolymers was examined by a combination of the GPC and on-line infrared (IR) spectrometer.

### 2.4. Sample preparation

The polymers obtained were pressed in a laboratory press at 463 K with a small amount of 2,6-di-*tert*-butyl *p*-cresol (BHT) as a thermal stabilizer. The thickness of the compression-molded samples was adjusted to suitable thickness for measurements.

### 2.5. Measurements

Differential scanning calorimetry (DSC) measurements were made using a Seiko DSC-200. The samples were heated to 473 K and kept for 5 min. Then the samples were cooled to 173 K at a cooling rate of  $10\text{ K min}^{-1}$  to ensure that the thermal history of the samples was similar. The data were collected during the following heating process from 173 to 473 K at a heating rate of  $10\text{ K min}^{-1}$ . The inflection point of the heat flow was defined as the glass transition temperature  $T_g$ .

Oscillatory shear moduli,  $G'$  and  $G''$ , were measured using a cone-plate type rheometer (Rheometrics Dynamic Stress Rheometer SR-2000) in the angular frequency  $\omega$  of  $1.0 \times 10^{-2}$  to  $4.0 \times 10^2\text{ s}^{-1}$ . The temperature ranged from 296 to 503 K. Measurements were carried out under a nitrogen atmosphere in order to avoid thermo-oxidative degradation. The time–temperature superposition was applied to frequency dependence of oscillatory moduli at different temperatures in an attempt to determine the linear viscoelastic properties over a wide range of time scales.

The temperature dependence of oscillatory tensile

Table 1  
Molecular characteristics for the samples

Sample	Comonomer	$\alpha$ -Olefin content		Molecular weight		
		(mol%)	(wt%)	$M_n \times 10^{-5}$	$M_w \times 10^{-5}$	$M_z \times 10^{-5}$
EHR25	1-Hexene	25.2	50.3	1.03	1.45	1.90
EHR33	1-Hexene	33.4	60.1	1.38	2.02	2.73
EHR40	1-Hexene	39.8	66.5	1.51	2.48	3.73
EHR51	1-Hexene	50.5	75.4	1.38	2.31	3.43
EPR37	Propylene	37.2	47.0	0.71	1.02	1.34

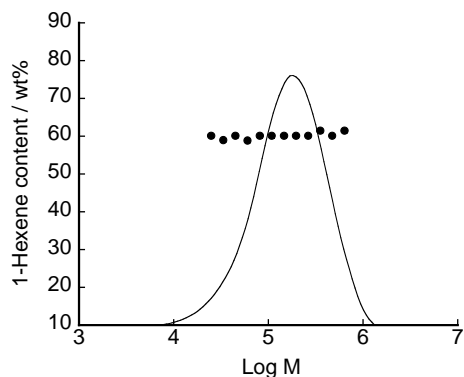


Fig. 1. GPC curve (solid line) and 1-hexene content (closed circles) of EHR33.

moduli,  $E'$  and  $E''$  was measured from 150 to 340 K at a heating rate of  $2 \text{ K min}^{-1}$  using a dynamic mechanical analyzer (Rheology, DVE V-4). The frequency used was 10 Hz. The rectangular specimens, in which the width is 1 mm, the thickness is 0.5 mm, and the length is 20 mm, were used. Density was measured at 296 K by means of a water–isopropanol density-gradient column.

### 3. Results and discussion

#### 3.1. Characteristics of polymers

The composition and the molecular weights of the copolymers used are shown in Table 1. As seen in the table, the 1-hexene content in EHR25 is as much as the propylene content in EPR37 by weight ratio. Moreover, the  $\alpha$ -olefin content in EPR37 is between those in EHR33 and EHR40 by molar ratio. Furthermore, all samples used have a high molecular weight and a narrow molecular weight distribution.

Fig. 1 exemplifies the result of the GPC-IR measurement of EHR33. As seen in the figure, the 1-hexene content in EHR33, denoted by closed circles, was constant irrespective of the molecular weight. All the copolymers used show similar results, which suggests that the samples have uniform comonomer incorporation.

Table 2 summarizes the monomer sequence distributions

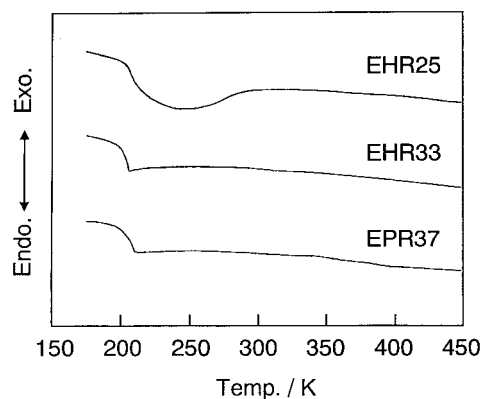


Fig. 2. DSC heating thermograms of EHR25, EHR33, and EPR37.

and reactivity ratios for the samples. As seen in the table,  $\alpha$ -olefin is incorporated randomly in the copolymers. The products of monomer reactivity ratios are around 0.25, therefore the copolymers have a somewhat alternating character.

Fig. 2 exemplifies the DSC heating thermograms. It is confirmed that all samples except for EHR25 have no crystalline phase. Only EHR25 shows a slight heat of fusion ascribed to the long chain sequence of the ethylene unit. The melting peak is, however, located below room temperature. Therefore, all samples including EHR25 show a rubbery state at room temperature. Moreover, the glass transition temperature can be detected as the inflection point, which will be discussed in the next section.

#### 3.2. Viscoelastic properties

Fig. 3 exemplifies the temperature dependence of tensile storage modulus  $E'$  and loss modulus  $E''$  conducted at 10 Hz. As seen in the figure, EHR25 shows a lower  $E'$  than EPR37 in the rubbery region. The result suggests that the rubbery plateau modulus  $G_N^0$  of EHR25 is lower than that of EPR37, which will be discussed in detail later. Furthermore, it is also found that the magnitude of  $E'$  above  $T_g$  decreases with increasing 1-hexene content for the EHRs. Moreover, a distinct peak due to the glass transition can be observed in the  $E''$  curve at the temperature region between 190 and 250 K. The  $T_g$ , peak temperature

Table 2  
Monomer sequence distribution for the samples

Sample	$\alpha$ -Olefin content (mol%)	Triad sequence distribution (%)						Diad (%)			$r_{E'}r_O^a$
		EEE	OEE + EEO	OEO	EOE	EOO + OOE	OOO	EE	EO	OO	
EHR25	25.2	36.8	30.1	7.9	21.9	2.0	1.3	51.9	45.8	2.3	0.23
EHR34	33.4	24.0	29.3	13.3	25.0	5.5	2.9	38.7	55.7	5.6	0.28
EHR40	39.8	15.6	27.8	16.8	25.9	9.6	4.3	29.5	61.4	9.1	0.28
EHR51	50.5	6.8	22.1	20.6	23.5	16.1	10.9	17.9	63.2	18.9	0.34
EPR37	37.2	17.8	28.2	16.8	25.0	9.8	2.4	31.9	60.8	7.3	0.25

<sup>a</sup>  $r_{E'}r_O = 4[EE][OO]/[EO]^2$ .

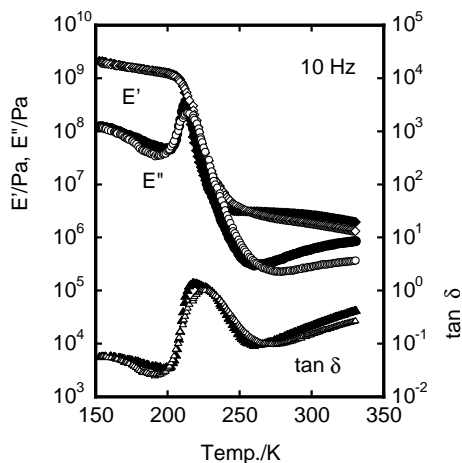


Fig. 3. Temperature dependence of storage modulus  $E'$  (diamonds), loss modulus  $E''$  (circles), and  $\tan \delta$  (triangles) for EPR37 (closed symbols) and EHR25 (opened symbols). The frequency used was 10 Hz.

of the  $E''$  curve, of EPR37, 212 K, is lower than that of EHR25, 215 K. As is well known,  $T_g$  depends on the species and the content of  $\alpha$ -olefin units.

According to Mäder et al. [6] and Carella et al. [7], EBR and EHR show the lowest  $T_g$  when the  $\alpha$ -olefin content is about 50–60 wt%. Fig. 4 shows the compositional dependence of the  $T_g$  for the EHRs used in this study. In the figure, the values of  $T_g$  obtained from the DSC measurements are also plotted. In general, the  $T_g$  depends on the frequency or time scale for the measurements. Therefore, the values from the DSC measurements are not identical to those from the dynamic mechanical measurements. Also in this experiment, EHR33 shows the lowest  $T_g$ . The result corresponds to the previous result obtained by EPR and EBR. However, much attention should be paid to discussing the phenomenon, because EHR25 has a crystalline phase whereas the other EHRs do not. Even though the degree of the crystallinity is low, the crystalline phase will act as the crosslink

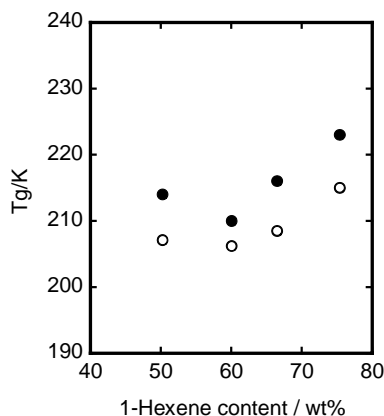


Fig. 4. Glass transition temperature  $T_g$  of EHRs with different 1-hexene content: (●)  $T_g$  obtained from dynamic mechanical measurements, and (○) from DSC measurements.

point and restrict the mobility of the amorphous phase. As a result, it enhances the glass transition temperature. Therefore, it is not appropriate that we discuss the compositional dependence of  $T_g$  for all samples including EHR25 from the scientific point of view. As far as this study goes, we can conclude that  $T_g$  increases with increasing  $\alpha$ -olefin content for the fully amorphous EHRs. Moreover,  $T_g$  of EHR33, 210 K, is lower than that of EPR37.

Fig. 5 shows the master curves of shear storage modulus  $G'$  and loss modulus  $G''$  of the copolymers. The reference temperature is 296 K. The curves show a terminal, rubbery plateau, and transition zones in the frequency range. The viscoelastic properties shown in Figs. 4 and 5 are those typical of amorphous polymers. Furthermore, the shift factor  $a_T$  obtained in this study can be expressed by the following WLF equation [11],

$$-\frac{T - T_r}{\log a_T} = -\frac{c_2}{c_1} + \frac{T - T_r}{c_1} \quad (1)$$

$$c_1 = B/2.303f_r \quad (2)$$

$$c_2 = f_r/\alpha_f \quad (3)$$

where  $f_r$  is the fractional free volume at reference temperature  $T_r$  and  $\alpha_f$  the temperature coefficient of the fractional free volume.

Assuming  $B = 1$ , we estimate the parameters of the samples. The results are summarized in Table 3. The magnitude of the  $\alpha_f$  of EPR37 is larger than that of the EHRs. It suggests that EPR37 shows a larger thermal expansion coefficient. The value of  $f_r$  is expressed as  $f_g + \alpha_f(T_r - T_g)$ , where  $f_g$  represents the free volume fraction at  $T_g$ . As is well known,  $f_g$  is almost independent of the polymer species [11]. Therefore, the polymer having a lower  $T_g$  and/or a larger  $\alpha_f$  exhibits a large value of  $f_r$ .

Moreover, we determine the rubbery plateau modulus  $G_N^0$  from the following equation [11]:

$$G_N^0 = \frac{2}{\pi} \int_{-\infty}^a G'' d \ln \omega \quad (4)$$

where  $a$  is the upper limit before the transition zone is entered.

Generally, the parameter can be obtained by the integration of  $G''$  over  $\ln \omega$  encompassing the maximum of  $G''$ .

Table 3  
WLF parameters (reference temperature is 296 K) for the samples

Sample	$c_1$	$c_2$	$f_r \times 10^3$	$\alpha_f \times 10^4$ (K <sup>-1</sup> )
EHR25	6.45	186	6.7	3.6
EHR33	6.01	143	7.2	5.0
EHR40	7.04	181	6.2	3.4
EHR51	6.90	171	6.3	3.7
EPR37	5.51	152	7.9	5.2

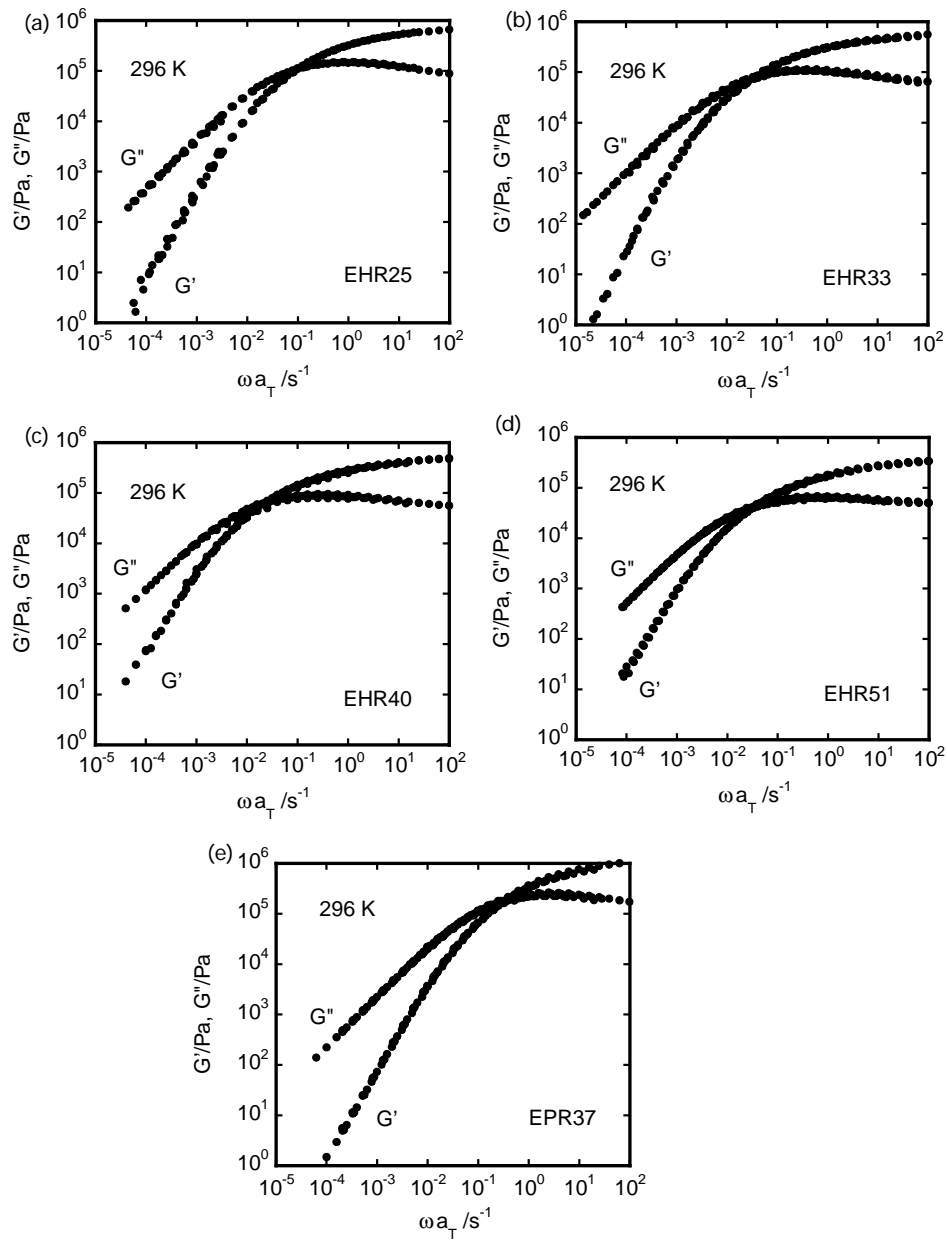


Fig. 5. Master curves of frequency dependence of shear storage modulus  $G'$  and loss modulus  $G''$  at 296 K: (a) EHR25, (b) EHR33, (c) EHR40, (d) EHR51, and (e) EPR37.

In this study, the  $G''$  versus  $\ln \omega$  curve was numerically integrated from  $\ln \omega = -\infty$  to the maximum of  $G''$ , and the result was doubled. It is well known that the average molecular weight between entanglement coupling by points ( $M_e$ ) is related to  $G_N^0$  as,

$$M_e = \frac{\rho RT}{G_N^0} \quad (5)$$

where  $\rho$  is the density.

As shown in Table 4,  $G_N^0$  decreases with increasing 1-hexene content in the EHRs. Moreover,  $G_N^0$  of EPR37, which agrees well with that reported previously [11], is

much higher than those of the EHRs used. Consequently, EPR37 exhibits a larger value of  $E'$  in Fig. 3.

According to Graessley and Edwards [12], the rubbery plateau modulus  $G_N^0$  is related with the average molecular

Table 4  
Rubbery plateau modulus  $G_N^0$  and average molecular weight between entanglement coupling by points  $M_e$  for the samples

Sample	$G_N^0$ (MPa)	$M_e$
EHR25	0.60	3500
EHR33	0.42	5000
EHR40	0.44	4800
EHR51	0.31	6800
EPR37	1.06	2000

weight per main chain bond  $m_0$  and characteristic ratio  $C_\infty$  by

$$G_N^0 \propto m_0^{-d} C_\infty^{2d-3} \quad (6)$$

$$m_0 = 14(1-x) + kx \quad (7)$$

$$C_\infty = nl_0^2 \quad (8)$$

where  $d$  is a constant,  $x$  the mole fraction of copolymer,  $k$  half of the molecular weight of the  $\alpha$ -olefin unit, and  $l_0$  the average length of the main chain bonds. Moreover, Graessley and Edwards [12] found that  $k$  takes the value 2.3 from the experimental results. Consequently,

$$G_N^0 \propto m_0^{-2.3} C_\infty^{1.3} \quad (9)$$

As seen in the relation,  $G_N^0$  will be more affected by the value of  $m_0$  than by that of  $C_\infty$ . Thus, assuming that the effect of  $C_\infty$  is negligible, we estimate  $G_N^0$  of the various ethylene/ $\alpha$ -olefin copolymers. According to Carella et al. [7],  $G_N^0$  of polyethylene is  $2.3 \times 10^6$  Pa at 463 K. Therefore,  $G_N^0$  at 296 K can be obtained by the following relation [7].

$$G_N^0(T_0) = G_N^0(T) b_T \quad (10)$$

$$b_T = \frac{\rho(T)^d T C_\infty(T)^{2d-3}}{\rho(T_0)^d T_0 C_\infty(T_0)^{2d-3}} \quad (11)$$

where  $T$  and  $T_0$  are 296 and 463 K, respectively.

The density of polyethylene at 463 K is  $760 \text{ kg m}^{-3}$  [13], and that of the amorphous region at 296 K is  $851 \text{ kg m}^{-3}$  [14]. Moreover, the value of  $C_\infty$  at 373 K is 7.2 [15]. Furthermore, the temperature dependence of  $C_\infty$  is given by the following relation [15].

$$\frac{d \ln C_\infty}{dT} = -1.1 \times 10^{-3} (\text{K}^{-1}) \quad (12)$$

As a result,  $b_T$  at 296 K is estimated to be 0.80. Therefore, we can decide that the magnitude of  $G_N^0$  at 296 K is  $1.85 \times 10^6$  Pa, assuming that polyethylene does not crystallize. Thus, we predict  $G_N^0$  of various ethylene/ $\alpha$ -olefin copolymers. Fig. 6 compares experimental values, denoted by circles, with the predicted ones, denoted by solid lines. In the figure, the values obtained by the preceding study, in which EHRs having 30 and 53 mol% of 1-hexene were employed [16], were also plotted. As seen in the figure, the experimental values agree well with the predicted ones, even though the effect of  $C_\infty$  is not taken into account. The compositional dependence of  $C_\infty$  was studied for some ethylene/ $\alpha$ -olefin copolymers [17,18]. In particular, the  $C_\infty$  of EBRs with various compositions has been studied experimentally [17]. In Fig. 6, the  $G_N^0$  predicted by relation (9), in which the effect of  $C_\infty$  is taken into account, is also shown by the dashed line. As seen in the figure, it is confirmed that the effect of  $C_\infty$  on  $G_N^0$  can be negligible.

Fig. 6 demonstrates that the magnitude of  $G_N^0$  can be easily predicted from the composition of copolymers. The

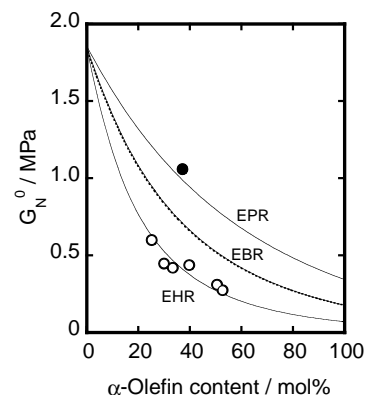


Fig. 6. Rubbery plateau modulus  $G_N^0$  for various rubbery ethylene/ $\alpha$ -olefin copolymers at 298 K. In the figure, circles denote the experimental values ( $\bullet$  EPR, and  $\circ$  EHRs), the solid lines the predicted values assuming that the effect of  $C_\infty$  is negligible, and the dashed line the predicted value in which the effect of  $C_\infty$  is taken into account.

results will help the design of ethylene/ $\alpha$ -olefin copolymers for industrial applications, because processability and mechanical properties are much affected by  $G_N^0$ .

#### 4. Conclusions

In the present study, the copolymerization of ethylene and 1-hexene was performed with diphenylmethylidene (cyclopentadienyl-fluorenyl) zirconium dichloride ( $\text{Ph}_2\text{C}(\text{Cp})(\text{Flu})\text{ZrCl}_2$ ) in combination with dimethylanilinium tetrakis-(pentafluorophenyl)borate ( $(\text{Me}_2\text{PhNH})(\text{B}(\text{C}_6\text{F}_5)_4)$ )/triisobutylaluminum ( $i\text{-Bu}_3\text{Al}$ ) catalyst. It was found that the catalyst system produced ethylene/1-hexene random copolymers (EHRs) with high molecular weight and narrow molecular weight distribution. Moreover, the 1-hexene content in the EHRs was constant irrespective of the molecular weight, suggesting that the EHRs have uniform comonomer incorporation. Furthermore, the product of monomer reactivity ratios is found to be around 0.25.

The EHR with 33 mol%, i.e. 60 wt%, of 1-hexene shows the lowest glass transition temperature  $T_g$  among the EHRs used. The  $T_g$  of the EHR is lower than that of the EPR having 47 wt% of propylene.

It was found from the rheological measurements that the rubbery plateau modulus  $G_N^0$  of the EHRs decreases with increasing 1-hexene content. Furthermore, the value of  $G_N^0$  is much lower than that of the EPR. Moreover, the magnitude of  $G_N^0$  can be predicted from the simple relation considering the average molecular weight per main chain bond.

#### References

- [1] Sinn H, Kaminsky W. Adv Organomet Chem 1980;18:99.
- [2] Kaminsky W, Miri M. J Polym Sci Polym Chem Ed 1985;23:2151.
- [3] Ewen JA. Ligand effects on metallocene catalyzed Ziegler–Natta

- polymerization. In: Keii T, Soga K, editors. Catalytic polymerization of olefins. Tokyo: Kodansya, 1986. p. 271.
- [4] Chien JCW, He D. *J Polym Sci Polym Chem Ed* 1991;29:1585.
- [5] Uozumi T, Soga K. *Macromol Chem* 1992;193:823.
- [6] Mäder D, Heinemann J, Walter P, Mülhaupt R. *Macromolecules* 2000;33:1254.
- [7] Carella J, Graessley WW, Fetters LJ. *Macromolecules* 1984;17:2775.
- [8] Razavi A, Atwood JL. *J Organomet Chem* 1993;459:117.
- [9] Hsieh ET, Randall JC. *Macromolecules* 1982;15:353 (see also p. 1402).
- [10] Grubisic Z, Rempp P, Benoit H. *J Polym Sci Polym Lett Ed* 1967;5:753.
- [11] Ferry JD. *Viscoelastic properties of polymers*. 3rd ed. New York: Wiley–Interscience, 1980.
- [12] Graessley WW, Edwards SF. *Polymer* 1981;22:1329.
- [13] Maloney DP, Prausnitz JM. *J Appl Polym Sci* 1974;18:2703.
- [14] Kitamaru R, Horii F, Hyon SH. *J Polym Sci Polym Phys Ed* 1977;15:821.
- [15] Flory PJ. *Statistical mechanics of chain molecules*. New York: Wiley–Interscience, 1969.
- [16] Yamaguchi M, Suzuki K, Miyata H. *J Polym Sci Polym Phys Ed* 1999;37:701.
- [17] Fetters LJ, Graessley WW, Krishnamoorti R, Lohse DJ. *Macromolecules* 1997;30:4973.
- [18] Reichart GC, Graessley WW, Register RA. *Macromolecules* 1998;31:7886.